Title
Discussion of "Single piles in lateral spreads: field bending moment evaluation"

Permalink
https://escholarship.org/uc/item/43w2p84w

Journal
Journal of Geotechnical and Geoenvironmental Engineering, 131(4)

ISSN
1090-0241

Authors
Brandenberg, Scott J
Boulanger, R W
Kutter, Bruce L

Publication Date
2005-04-01

Peer reviewed

Discussion of "Single Piles in Lateral Spreads: Field Bending Moment Evaluation" by Ricardo Dobry, Tarek Abdoun, Thomas D. O'Rourke, and S.H. Goh

Scott J. Brandenberg[1]; Ross W. Boulanger[2]; and Bruce L. Kutter[3]

[1]Graduate Student, Univ. of California, Davis, Dept. of Civil and Environmental Engineering, Davis, CA 95616, E-mail: sjbrandenberg@ucdavis.edu

[2]Professor, Univ. of California, Davis, Dept. of Civil and Environmental Engineering, Davis, CA 95616.

[3]Professor, Univ. of California, Davis, Dept. of Civil and Environmental Engineering, Davis, CA 95616.

The authors should be commended on their contribution to the study of pile foundations in liquefied and laterally spreading ground. The data collected in their centrifuge tests and their subsequent analyses contribute to the understanding of soil-pile interaction during liquefaction-induced lateral spreading. An analytical model based on limit equilibrium (LE) and elastic solutions (referred to as an LE model) for predicting bending moments in single piles subjected to loads from a laterally spreading crust was calibrated with centrifuge test data presented in a companion paper (Abdoun et al. 2003). The flexible pile foundation in centrifuge Model 1 experienced head displacements that would be considered too large in most design applications. The applicability of the LE model for stiffer piles that would exhibit satisfactory behavior in lateral spreads with a crust was left unexplored. In particular, the limiting state for $z_{ps}=0$ was not observed in the centrifuge tests and was not highlighted in the associated LE solutions. Comparisons of LE and beam on nonlinear Winkler foundation (BNWF) analyses for stiffer piles are used in this discussion to bring attention to the practical importance of this limiting state and supplement the utility of the authors' methodology.

Characterization of Observed Loading Mechanics for Flexible Pile in Model 1

Centrifuge Model 1 contained a single pile (diameter, d =0.60 cm, EI=8,000 kN·m^2) in a soil profile consisting of a nonliquefiable cemented sand crust over liquefiable loose sand over nonliquefiable cemented sand. As the crust spread laterally on top of the liquefiable sand, it caused a gripping action on the pile in which the crust below a transition depth z_{ps} pushed the pile downslope, and the crust above z_{ps} restrained the pile from moving downslope. When crust displacement D_H was 0.29 m, the pile head "snapped" downslope through the nonliquefied crust, which verified the gripping action on the pile. The direction of subgrade reaction loading is controlled by the direction of relative displace-

ment between the free-field soil and the pile, so the gripping action is associated with a pile head displacement that is larger than the free-field ground surface displacement.

The LE model was calibrated to the test data by assuming elastic perfectly plastic soil-pile interaction behavior such that the evolution of bending moment with increasing D_H is approximately bilinear (see Fig. 7 in the original paper). The values of M_A, M_B, H_A (shear force at point A), and z_{ps} are calculated in the original paper by simultaneously solving Eqs. (3), (4), (5), and (6) at the yield point and Eqs. (3), (4), (5), and (9) after the yield point. At the yield point, the ultimate subgrade reaction is mobilized against the pile in the downslope direction below z_{ps} and in the upslope direction above z_{ps}. As D_H increases after yield, z_{ps} gradually shifts upward (decreases in magnitude) such that a larger portion of the crust exerts downslope loading on the pile, which causes M_A to linearly decrease and M_B and H_A to linearly increase. The model was calibrated out to the peak crust displacement for the centrifuge test D_H=0.8 m, at which point the predicted moments (M_A=142 kN·m, M_B=356 kN·m) match reasonably well with the measured data ($M_A \approx 140$ kN·m, M_B =305 kN·m). The model predicts z_{ps}=1.29 m at D_H=0.80 m, which is only a slight decrease over z_{ps}=1.34 m at the yield point.

Limiting State When $z_{ps}=0$

The LE model reaches a limiting state when $z_{ps}=0$ because the transition depth must lie somewhere within the soil layer. This limiting state did not develop for the flexible pile in centrifuge Model 1 but is of practical interest for stiffer piles, as will be shown subsequently. Although the limiting state can be found by simultaneously solving Eqs. (3), (4), (5), and (9) in the original paper for different values of D_H until $z_{ps}=0$, the limiting bending moments ($M_{A,\text{lim}}$ and $M_{B,\text{lim}}$) limiting shear load at point A ($H_{A,\text{lim}}$) and ground surface displacement at the limiting state ($D_{H,\text{lim}}$) can be more easily calculated by setting $\alpha = z_{ps}/h = 0$ in Eqs. (3) and (4), then solving Eqs. (5) and (9). The resulting equations are

$$\frac{M_{A,\text{lim}}}{p_0 \cdot h^3} = -\frac{1}{6} \tag{1}$$

$$\frac{H_{A,\text{lim}}}{p_0 \cdot h^2} = \frac{1}{2} \tag{2}$$

$$\frac{M_{B,\text{lim}}}{p_0 \cdot h^3} = \frac{L}{2 \cdot h} + \frac{1}{6} \tag{3}$$

$$\frac{EI}{p_0 \cdot h^3 \cdot L^2} \cdot D_{H,\text{lim}} = \frac{L}{6 \cdot h} + \frac{1}{12} + \frac{EI}{k_r \cdot L} \cdot \left(\frac{L}{2 \cdot h} + \frac{1}{6} \right) \tag{4}$$

For practical purposes, knowing the values of M_A, M_B, and D_H at the yield point from Eqs. (3), (4), (5), and (6) in the original paper and at the limiting point from Eqs. (1)–(4) in this discussion is sufficient to characterize the relationship of moment versus crust displacement because its shape is approximately trilinear.
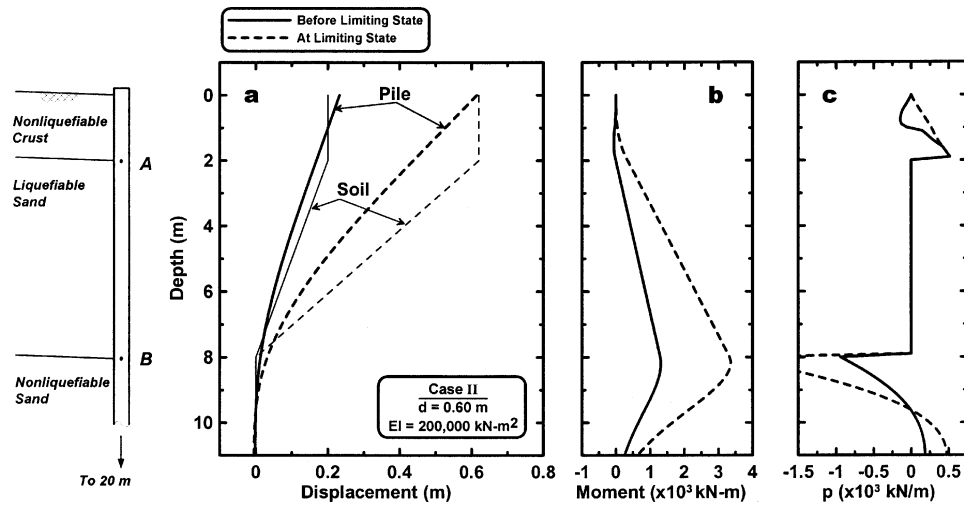
Fig. 1. Results of (a) displacement; (b) bending moment; and (c) subgrade reaction from Case II BNFW analyses before and at the limiting state

Beam on Nonlinear Winker Foundation Analyses

Application of the authors' LE model to stiffer piles is illustrated by comparing it to results of BNWF analyses with imposed free-field soil displacements performed using LPile+4.0 m (Reese et al. 2000) for three different pile foundations. The soil profile and *p-y* elements used in the BNWF analyses were calibrated to match observations from centrifuge Model 1. The first BNWF analysis, Case I, contained a pile with the same properties as that used in centrifuge Model 1 ($d=0.60$ m, $EI=8,000$ kN·m^2). The Case II pile had the same diameter as the pile in Case I but a larger flexural stiffness ($d=0.60$ m, $EI=200,000$ kN·m^2), and Case III contained a stiffer, larger diameter pile ($d=1.25$ m, $EI=2,750,000$ kN·m^2). For all three cases, the piles were treated as linear elastic, and the pile length was extended to a depth of 20 m because only 2 m of embedment into the underlying nonliquefied layer, as existed in centrifuge Model 1, would result in rotational failure at the tips of the stiffer piles.

Fig. 1 in this discussion shows the BNWF analysis results for Case II with ground surface displacements of 0.2 and 0.62 m. The ground surface displacement of 0.62 m produces the limiting state at which the pile head displacement equals the ground surface displacement, and the crust layer is applying passive downslope pressures over its full thickness (i.e., $z_{ps}=0$). Further increases in ground surface displacement cause no changes in the pile displacements, bending moments, or lateral soil pressures. At smaller ground displacements (e.g., the 0.20 m case shown in Fig. 1 in this discussion), the pile head displacement is larger than the ground surface displacement, as expected.

Case I Comparison

The ground surface in the Case I BNWF analysis was pushed to a very large displacement of 10 m to illustrate the theoretical limiting state, although the results are physically meaningless because the BNWF (and LE) analyses neglect large deformation effects. Fig. 2(a) in this discussion contains the results of the BNWF analyses plotted together with the response predicted by the LE model. The results show good agreement, with both analyses predicting that the limiting state is reached when the ground displacement is larger than about 8.5 m. Note that the sign convention for M_A in Fig. 2 in this discussion follows the authors'

sign convention (Fig. 6), which is opposite to that shown in Fig. 1 in this discussion (the sign conventions for M_B are the same, however).

Case II Comparison

The ground surface in Case II was pushed to a displacement of 1.0 m, and the limiting state was reached at $D_{H,\lim}=0.62$ m. Fig. 2(b) in this discussion shows good agreement between the BNWF results and the LE model prediction, though the LE model predicts a smaller limiting displacement $D_{H,\lim}=0.56$ m. The rotational spring stiffness, k_r, for the LE analysis was scaled from the authors' value for the $EI=8,000$ kN·m^2 pile using an elastic solution of a laterally-loaded vertical pile with consideration for rotations induced by an applied shear and moment. The two analysis methods show that once the pile deflects about 0.6 m, it can resist the passive loads exerted by the crust as it spreads downslope around the pile.

Case III Comparison

The ground surface for the Case III pile was again pushed to a displacement of 1.0 m, but the limiting state was reached after only 0.16 m of displacement. The rotational spring k_r for the LE analysis was again estimated using an elastic solution. Fig. 2(c) in this discussion shows good agreement between the BNWF results and the LE model prediction, and both analyses predict that a pile head displacement of 0.16 m would be required to resist the passive loads from the laterally spreading crust.

Discussion

The LE and BNWF analysis results shown in Figs. 1 and 2 in this discussion illustrate how pile foundations can reach a limiting state where the crust exerts downslope passive pressures over its full thickness. This limiting state defines the maximum magnitude of bending moment and pile displacement that will occur as the crust spreads past the piles. For cases where lateral spreading displacements are larger than the allowable pile head displacement, the limiting state will govern, and Eqs. (1)–(4) in this discussion provide a convenient means for obtaining a solution.
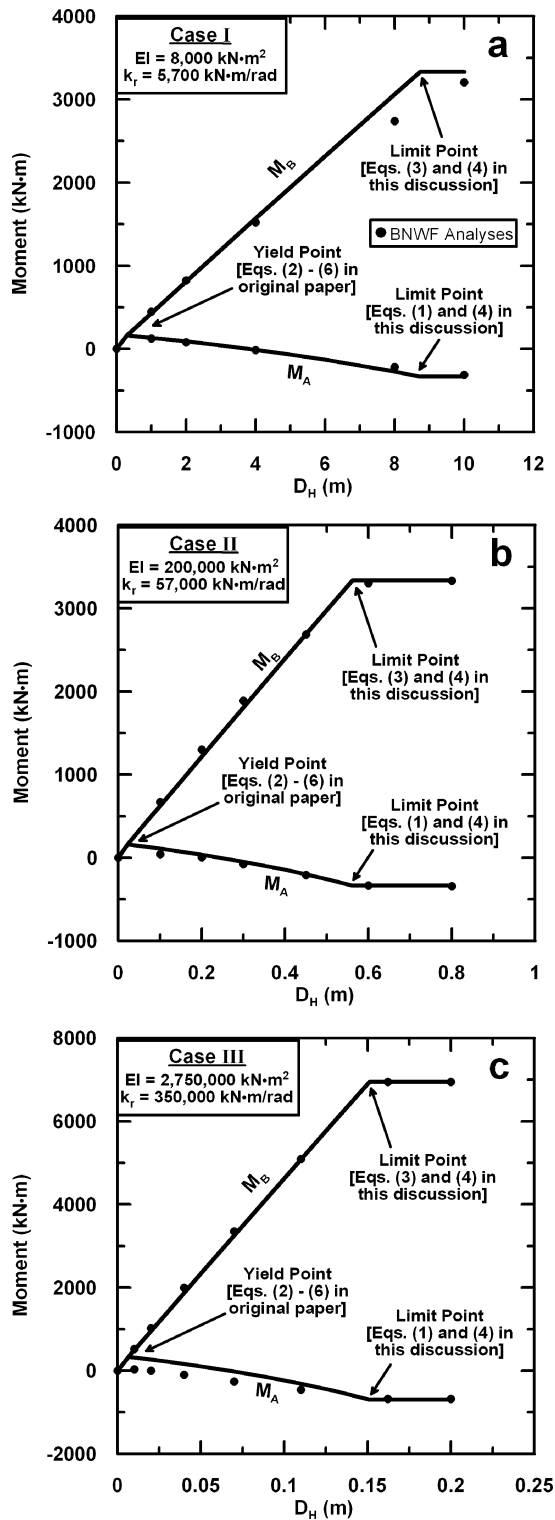
Fig. 2. M_A and M_B versus D_H from the modified LE model and from the BNWF analyses for (a) Case I; (b) Case II; and (c) Case III

may be partly attributed to the sand's low relative density, the pile's flexibility, and the modest levels of shaking. For many situations, the total lateral loads from a liquefied sand layer are of secondary importance to the total lateral loads from the overlying nonliquefied layers, and thus, a rough estimate of p_ℓ may be satisfactory. For example, including $p_\ell = 10$ kPa (as reported for some of the authors' other centrifuge tests) in the LE analysis for Case II in Fig. 1 in this discussion would increase the limiting bending moment near point B from 3333 kN·m to 3441 kN·m or only about 3%. Nonetheless, the dynamic centrifuge model tests by Wilson et al. (2000) and Boulanger et al. (2003) have shown that the dynamic lateral loads from liquefied sand can be an order of magnitude larger and not necessarily in phase with lateral crust loads and superstructure inertial loads, as is often assumed in simplified design procedures. The complexity of this behavior illustrates the limitations inherent to simplified design procedures and the necessity for caution in extrapolating analytical models beyond the ranges of their experimental validation.

It is also worth noting that $P \cdot \Delta$ effects can be an important consideration in situations involving large pile head displacements (e.g., Bhattacharya and Bolton 2004). Suppose that each of the piles in Fig. 2 in this discussion were carrying an axial load of 450 kN and that axial skin friction in the liquefiable sand is negligible. For a ground surface displacement of 1 m, the BNWF results indicate that the additional bending moment at point B due to $P \cdot \Delta$ effects would be about 518 kN·m (450 kN times 1.15 m) for Case I, 279 kN·m (450 kN times 0.62 m) for Case II, and 72 kN·m (450 kN times 0.16 m) for Case III. These $P \cdot \Delta$ effects represent 104, 8, and 1% increases in M_B for Cases I, II, and III, respectively. This illustrates how $P \cdot \Delta$ effects can be very important for flexible piles but relatively insignificant when larger diameter piles are used to limit pile-head deflections to more reasonable levels.

The authors' work has contributed toward improved design methodologies for pile foundations in areas of liquefaction and lateral spreading. It is hoped that this discussion of the LE model provides a useful supplement to their efforts.

References

Abdoun, T., Dobry, R., O'Rourke, T. D., and Goh, S. H. (2003). "Pile response to lateral spreads: Centrifuge modeling." *J. Geotech. Geoenviron. Eng.*, 129(10), 869–878.

Bhattacharya, S., and Bolton, M. D. (2004). "A fundamental omission in seismic pile design leading to collapse." *Proc., 11th Int. Conf. Soil Dynamics Earthquake Engineering, 3rd Int. Conf. Earthquake Geotechnical Engineering,* Univ. of California, Berkeley, Calif.

Boulanger, R. W., Kutter, B. L., Brandenberg, S. J., Singh, P., and Chang, D. (2003). Pile foundations in liquefied and laterally spreading ground during earthquakes: Centrifuge experiments and analyses. Rep. *UCD/CGM-03/01*, Center for Geotechnical Modeling, Univ. of California, Davis, Calif.

Haigh, S. K. (2002). "Effects of earthquake-induced liquefaction on pile foundations in sloping ground." PhD dissertation, Cambridge Univ., Cambridge, U.K.

Reese, L. C., Wang, S. T., Isenhower, W. M., Arrelaga, J. A., and Hendrix, J. A. (2000). "*LPILE Plus Verion 4.0m*, Ensoft, Inc. Austin, Tex.

Wilson, D. W., Boulanger, R. W., and Kutter, B. L. (2000). "Observed seismic lateral resistance of liquefying sand." *J. Geotech. Geoenviron. Eng.*, 126(10), 898–906.

Other centrifuge tests have shown that the lateral loads (or resistances) that develop between piles and liquefied sands are strongly dependent on a number of factors, including pile stiffness, relative density, foundation stiffness, and ground-motion characteristics (e.g., Wilson et al. 2000; Haigh 2002; Boulanger et al. 2003). With regard to the authors' centrifuge tests, the observation of negligible lateral pressures within the liquefied sand

Closure to "Single Piles in Lateral Spreads: Field Bending Moment Evaluation" by Ricardo Dobry, Tarek Abdoun, Thomas D. O'Rourke, and S. H. Goh

Ricardo Dobry[1]; Tarek Abdoun[2]; Thomas D. O'Rourke[3]; and S. H. Goh[4]

[1]Professor, Dept. of Civil Engineering, Rensselaer Polytechnic Institute, Troy, NY 12180-3590. E-mail: dobryr@rpi.edu

[2]Assistant Professor, Dept. of Civil Engineering, Rensselaer Polytechnic Institute, Troy, NY 12180-3590.

[3]Professor, School of Civil and Environmental Engineering, Cornell Univ., Ithaca, NY 14853-3501.

[4]Engineer, Mueser Rutledge Consulting Engineers, NY 10017.

We thank the discussers for their excellent contribution, which expands on the analytical approach proposed in our paper for an elastic pile when a nonliquefiable soil crust is present. They do that by covering a wider range of values of free field displacement D_H, and demonstrating that when D_H is large enough, $\alpha = z_{ps} = 0$, and a limiting plastic state develops that does not change for greater D_H. This limiting state provides upper-bound values $M_{A,\lim}$, $M_{B,\lim}$, and $H_{A,\lim}$ for the bending moments and shear force, which are of great interest to design, especially in the case of stiffer piles as illustrated by their Cases II and III (Figs. 1–2). Their proposed trilinear plots included in their Fig. 2 provide significant insight on the evolution of M_A and M_B as D_H increases, showing both the appearance of the local maximum $(M_A)_{\max}$ detected by the writers as well as the absolute maximum values $M_{A,\lim}$ and $M_{B,\lim}$. Their comparisons with state-of-practice program LPile$^+$4.0m constitute additional validation of the method and of the trilinear plots.

Therefore, Eqs. (2)–(9) in the original paper and Eqs. (1)–(4) in the discussion provide a unified set of expressions for development of the trilinear plots for M_A and M_B versus D_H when it is reasonable to expect that $M_A \approx M_B$ at small values of D_H (first leg of the trilinear plot). This may happen, for example, if the crust layer has approximately the same thickness and properties as the nonliquefiable soil penetrated by the pile below the liquefiable layer. That was the case of centrifuge Model 1 analyzed in the paper, where both were slightly cemented, 2-m-thick sand layers. However, there may be other situations where the properties of the two soils and/or their thicknesses are very different; in which case, the rotational pile stiffnesses k_{rA} and k_{rB} at points A and B will be different, and, hence, M_A and M_B will also be different from the beginning. In Eqs. (2) and (6)–(9) in the paper, the assumption is that $k_r = k_{rA} = k_{rB}$, and thus, $M = M_A = M_B$, and the value of the local maximum $(M_A)_{\max}$ calculated by Eqs. (7) and (8) in the paper depends on this assumption.

The method and trilinear plot concept can be easily expanded to the case in which the bending moments at A and B are different at small D_H because $k_{rA} \neq k_{rB}$. In that case, Eqs. (2) and (6)–(8) are replaced by the following:

$$M_A = \frac{D_H}{L[(L/6EI)(2\beta - 1) + (\beta/k_{rB})]} \quad (1a)$$

$$M_B = \frac{D_H}{L[(L/6EI)(2 - 1/\beta) + (1/k_{rB})]} \quad (1b)$$

$$M_B/M_A = \beta = \frac{1/k_{rA} + L/2EI}{1/k_{rB} + L/2EI} \quad (2)$$

$$3[1 + (1 + \beta)/(L/h)][(M_A)_{\max}/(p_0 h^3)]$$
$$= 1 - 2\{0.5 - [(1 + \beta)/(L/h)][(M_A)_{\max}/(p_0 h^3)]\}^{1.5} \quad (3)$$

$$(M_A)_{\max} \approx p_0 h^3/[10.23 + 3(1 + \beta)/(L/h)] \quad (4)$$

with all the above equations reducing to the corresponding expressions in the paper for the special case of $\beta = M_B/M_A = 1$. In the general case, where typically $\beta \neq 1$, Eq. (9) in the paper is still valid if k_r is replaced by k_{rB}.

It is interesting that in this case of unequal nonliquefiable layers in which $\beta \neq 1$ and the bending moments M_A and M_B are different from the beginning, only the first leg of the trilinear plots and the value of the local maximum $(M_A)_{\max}$ are affected, but the second and third legs of the trilinear plot, including the limiting state brought up by the discussers, are not affected at all. That is, Eqs. (3)–(5) and (9) in the original paper and Eqs. (1)–(4) in the discussion can be used irrespective of the value of β, provided that k_r is interpreted as k_{rB} in Eq. (9) and in Eq. (4) in the discussion. For the case of $M_B > M_A$ (i.e., $k_{rB} > k_{rA}$ and $\beta > 1$), the value of $(M_A)_{\max}$, computed with the original Eqs. (7) or (8), provides a conservative answer compared to the true value of $(M_A)_{\max}$ from Eqs. (3) or (4) here, while the opposite is true if $M_A > M_B$.

The discussers' contribution plus the above extension of the model to the case of unequal bending moments at low D_H provide a comprehensive picture of the kinematic response to lateral spreading as D_H increases of a single elastic pile embedded in a 3-layer sandy soil profile such as idealized in Fig. 6. The model has a number of limitations, some of which were pointed out by the discussers. It is limited to a sandy crust or similar soil with strength increasing with depth. It does not include the effect of the pile cap tested in centrifuge Model 2 of the paper. It is limited to single piles and, hence, is not applicable to pile groups. It does not include the effect of the superstructural lateral and rotational stiffnesses above ground acting at the pile head, which, as demonstrated by Ramos (1999) and Dale (2002), may have a profound influence on pile response. (A significant superstructure's lateral stiffness makes $z_{ps} = 0$ from the beginning, and thus, there is no local maximum $(M_A)_{\max}$ before the limiting state is reached.) The P-Δ effect as well as dynamic effects during shaking must be considered separately. These dynamic effects may arise either from inertial loads above ground (influencing mainly the pile bending moments within the crust), or as suggested by the discussers, from possible dynamic kinematic effects inducing dynamic pressures of the liquefied layer against the pile, which may indeed become more significant for liquefiable sand layers of higher relative density, stiffer piles, and/or greater levels of shaking. Finally, there are a couple of limitations related to Eq. (9) in the original paper and Eq. (4) in the discussion. One is the inability of Eq. (9) and Eq. (4) in the discussion to predict accurately the intersections between second and third legs of the trilinear plots at very large displacements D_H in flexible piles. As pointed out by the discussers, this happens because the two expressions neglect large deformation effects. A second potential limitation arises from the simplifying assumption in Eq. (9) and Eq. (4) in the discussion that $D_{pA} = D_H$, with the pile and soil displacements assumed equal at point A. This simplification becomes less defensible for stiffer piles and values of D_H approaching the limiting state, as illustrated for Case II in Fig. 1a of the discussion. Therefore, the writers add their voice to that of the discussers in rec-

ommending caution and good judgment when using the method, as should always be the case when applying a relatively simplified approach to a complex reality.

Another limitation of the method lies in its assumption that the pile behaves elastically at any value of D_H, reflected in the use of a constant value of EI which is independent of D_H and hence independent of the level of bending moment M acting on the pile section. Although this is approximately true for many steel piles, provided that the pile does not experience ultimate bending failure, it is generally not true for sections of reinforced concrete (RC) piles, for which the moment-curvature (M-ψ) plot is nonlinear starting at low values of the moment, caused by progressive concrete cracking, steel reinforcement yielding, and concrete crushing (Meyerhson 1994; O'Rourke et al. 1994; Cubrinovski and Ishihara 2002; Cubrinovski et al. 2004). As a result, the value of the secant EI in concrete piles decreases as M increases. An example is provided in Table 4 for the two NFCH piles considered in Niigata. While the ultimate bending moment capacity for Pile 2 listed in the table is estimated at 86 kN·m, the value of EI starts decreasing due to concrete cracking when the bending moment reaches about 18 kN·m. The initial, elastic bending stiffness of this pile is $EI \approx 20,000$ kN·m² up to this cracking moment, but the secant value of bending stiffness at a higher $M=40$ kN·m (about half of the ultimate moment capacity of the pile section) has decreased it to $EI \approx 8,000$ kN·m². This is why the writers selected a prototype $EI=8,000$ kN·m² for their centrifuge model piles, in an effort to approximately simulate with a linear pile model having an average EI, the global nonlinear response of this RC pile foundation under the Niigata NFCH building. Another source of nonlinearity occurs if the RC pile fails in shear, as happened to Pile 2 at point A (Fig. 1 in the paper), with the subsequent inability to transmit higher values of the shear force H_A after this failure. This observed pile shear failure is the reason why when applying the method to NFCH Pile 2 in Table 4 the writers took a factor-of-safety approach rather than trying to predict in detail the development of moments M_A and M_B as D_H increased. This evaluation in Table 4 used the local maximum $(M_A)_{\max}=198-400$ kN·m from Eqs. (7) and (8) in the paper to define the calculated factors of safety. The alternative of using the limiting state, i.e., the absolute maximum $M_{a,\lim}$ from Eq. (1) in the discussion instead of $(M_A)_{\max}$, is not appropriate because, in this case, the development of $M_{a,\lim}$ requires D_H to reach about 8.5 m, much more than the actual ground displacement measured near the NFCH building after the earthquake, $D_H=0.5$ to 2 m. Therefore, using $M_{A,\lim}=417-720$ kN·m computed from Eq. (10) in the discussion for the evaluation would have been too conservative given the known circumstances of this case history.

A possible way to circumvent the limitation of variable EI for RC piles, in cases when the estimated free field D_H at the end of the earthquake is still much less than $D_{H,\lim}$ from Eq. (4) in the discussion and a prediction is needed of the evolution of pile bending moments and shear force as D_H increases, could be to combine the method with an equivalent linear approach for EI. That is, the actual M-ψ curve of the pile section (including the corresponding unloading branch of the curve for M_A after $(M_A)_{\max}$) would be used together with the equations of the method, varying EI in the equations for a given D_H until the EI used is consistent with the secant EI value corresponding in the curve to bending moment M_A or M_B. Although this is more complicated that direct use of the trilinear plots and of Eqs. (7) and (8) in the paper and Eqs. (3) and (4) here, it may still be a practical way to predict bending moments, shear force, and, generally, pile section performance (initiation of concrete cracking, of steel

yielding, etc.) as D_H increases. A similar equivalent linear approach for RC piles has been suggested by Cubrinovski and Ishihara (2002).

The discussers make the point that the flexible pile foundation in centrifuge Model 1, $EI=8,000$ kN·m² (and also NFCH Pile 2 in Niigata with initial $EI \approx 20,000$ kN·m² and representative secant $EI \approx 8,000$ kN·m²) experienced head displacements that would be considered too large in most design applications. This is certainly true. It is also true that in current seismic design of new structures, piles tend to be stiffer than those we tested in the centrifuge and also stiffer than the piles present under the NFCH building. However, their Cases II and III covering a range of EI $=200,000-2,750,000$ kN·m² are quite stiff, larger than values of EI relevant to a number of practical applications. This becomes apparent when considering both seismic retrofitting of older vintage, small diameter pile foundations and the need to use a reduced secant value of EI in many cases of RC piles for the calculations due to M-ψ nonlinearity, as discussed previously. Published charts for bridge foundation seismic pile design (Lam et al. 1998) cover a wide range of EI between about 10^9 and 10^{13} lb·in.² (2,870 to 28,700,000 kN·m²) and a 12-in.-square concrete pile often encountered in retrofitting studies (Lam, personal communication, 2004), has an initial $EI \approx 18,000$ kN·m², which, as discussed previously, is further reduced as the bending moment increases. Therefore, a very wide range of values of EI is present in seismic foundation engineering practice, from very flexible piles and low EI as considered by the writers and exemplified by Case I, to much stiffer piles and high EI as pointed out by the discussers and exemplified by Cases II and III. Although it is true that centrifuge Model 1 (Case I) experienced head displacements close to 1 m, that would be considered too large in most new design applications, the current tendency, especially when dealing with expensive retrofitting of existing foundations, is toward performance-based design where an attempt is made to predict the actual performance of the foundation and structure above ground for various scenarios of retrofitting (or nonretrofitting). In our opinion, the method developed in the paper, discussion, and closure, provides a good analytical framework for engineers interested in predicting the actual performance of single piles to lateral spreading as D_H increases in the free field. The approach works best for relatively flexible piles, which have been used frequently in foundation systems. The approach can be adapted to nonlinear M-ψ characteristics, typical of RC piles, with equivalent linear procedures for estimating EI.

In some cases, the engineer may also want to refine the method by replacing Eq. (9) and Eq. (4) in the discussion by more complicated versions in order to remove the simplifying assumption of $D_{pA}=D_H$ in cases of stiff piles and high D_H for which the assumption is not realistic or to introduce large deformation effects at very high D_H. These refinements can be made with the analytical framework that now includes the very useful trilinear plot concept introduced by the discussers. On the other hand, we do agree with the discussers that there are many applications related to the design of new pile foundations in which high pile stiffness combined with a limited allowable pile head displacement can be solved with their simplified assessment of the trilinear plot. In such cases, the engineer can go directly to the limiting plastic state defined by the discussers in Eqs. (1)–(4).

References

Cubrinovski, M., and Ishihara, K. (2002). "Pile response to lateral spreading of liquefied soils: Demand-capacity method." *Proc., U.S.-Japan Workshop on Seismic Disaster Mitigation in Urban Areas by Geotechnical Engineering*, Anchorage, Alaska, June, paper 4–4.

Cubrinovski, M., Kokusho, T., and Ishihara, K. (2004). "Interpretation of large-scale shake table tests on piles subjected to spreading of liquefied soils." *Proc., 11th Int. Conf. Soil Dynamics and Earthquake Engng., and 3rd Int. Conf. on Earthquake Geotechnical Engineering*, Univ. of California, Berkeley, Calif., 2, 463–470.

Dale, G. R. (2002). "Prediction of pile bending response to lateral spreading by elastoplastic analysis validated by centrifuge tests." MS thesis, Dept. of Civil and Environmental Engineering, Rensselaer Polytechnic Institute, Troy, N.Y.

Lam, I. P., Kapuskar, M., and Chaudhuri, D. (1998). "Modeling of pile footings and drilled shafts for seismic design." *Tech. Rep. MCEER-98-0018*, Multidisciplinary Center for Earthquake Engineering Research, State Univ. of New York at Buffalo, Buffalo, N.Y.

Meyersohn, W. D. (1994). "Pile response to liquefaction induced lateral spread." PhD thesis, Dept. of Civil and Environmental Engineering, Cornell University, Ithaca, N.Y.

O'Rourke, T. D., Meyersohn, W. D., Shiba, Y., and Chaudhuri, D. (1994). "Evaluation of pile response to liquefaction-induced lateral spread." *Proc.,5th U.S.-Japan Workshop on Earthquake Resistant Design of Lifeline Facilities and Countermeasures Against Soil Liquefaction*, NCEER 94-0026, National Center for Earthquake Engineering Research, Buffalo, N.Y., 457–480.

Ramos, R. (1999). "Centrifuge study of bending response of pile foundation to a lateral spread including restraining effect of superstructure." PhD thesis, Dept. of Civil Engineering, Rensselaer Polytechnic Institute, Troy, N.Y.